Estimating the escape zone for a parametrically excited pendulum-type equation

I. W. Stewart[1] and T. R. Faulkner[2]
[1]*Department of Mathematics, University of Strathclyde, Livingstone Tower, 26 Richmond Street, Glasgow G1 1XH, United Kingdom*
[2]*Division of Theoretical Mechanics, School of Mathematical Sciences, University of Nottingham, University Park, Nottingham NG7 2RD, United Kingdom*
(Received 29 February 2000)

This paper derives theoretical results for determining bifurcation curves which provide bounds on anticipated ''escape'' regimes in a two-dimensional parameter space for an equation which is a natural extension of a commonly used second-order parametrically excited nonlinear pendulum equation. An application of these results is made for an equation which often arises in smectic liquid-crystal problems. The results for this application are more refined yet qualitatively similar to those obtained by different methods reported in the literature.

PACS number(s): 05.45.−a, 61.30.Cz

I. INTRODUCTION

A study will be made of the equation

$$\ddot{\phi}+2\xi\dot{\phi}+[1+p\cos(\omega t)][\sin\phi+a\sin(2\phi)]=0, \tag{1.1}$$

where ξ, p, ω, and a are constants and ϕ is a time-dependent function which has its derivative with respect to time denoted by a superposed dot. Equation (1.1) for $a\neq 0$ is motivated by the dynamic equations which often appear in the smectic liquid-crystal literature that have sinusoidal nonlinearities similar to the double sine-Gordon equation. A short summary of such equations may be found in Stewart [1] and in the articles mentioned below as they become relevant. The usual parametrically excited pendulum equation is recovered from Eq. (1.1) by setting $a=0$. The analysis employed below is motivated by the work of Clifford and Bishop [2] and Capecchi and Bishop [3] who considered the parametrically excited pendulum form of Eq. (1.1) for small fixed $\xi>0$ when $a=0$; a harmonic balance criterion was used for determining approximations for the location of an ''escape'' region in the corresponding p, ω plane. For many applications it is known that predicting parameter regions where no major stable nonrotating orbits exist is of primary importance and under these circumstances the parametrically excited pendulum is analogous to a system that allows escape from a potential well. Escape parameter regions and chaotic behavior have been studied extensively for the parametrically excited pendulum [2–7] and it is our aim to extend these basic ideas to Eq. (1.1) for fixed ξ and $a\neq 0$. The initial results we pursue in Sec. II enable us to suggest an approximate location for the escape parameter region in the p,ω plane for Eq. (1.1). These results are then interpreted in Sec. III in the context of a particular application which arises in the smectic liquid-crystal literature involving a special approximation to a perturbation of a dynamic equation. The work presented here therefore naturally extends the nonlinear work for the parametrically excited pendulum cited above and is further illustrated by means of this application. Numerical determination of the escape regions for the cases discussed below remains to be investigated fully: it is intended that these preliminary results will encourage future numerical work by providing guidance as to the location of the actual escape regions. An initial numerical investigation for Eq. (1.1) has been carried out recently by Clifford [8] who has confirmed the location and accuracy to within two or three decimal places of the boundary of the escape region depicted in Fig. 1 below when $a=0.3$ and $\omega\approx 2$. The first indications are that the full extent of the rich nonlinear behavior available to solutions of this equation will require quite extensive and detailed numerical investigations which will be reported in future work.

II. HARMONIC BALANCE METHOD

We follow [2] and try to approximate the escape zone boundary by means of identifying two bifurcations. As in [2,3], it will be assumed that the symmetry-breaking bifurcation derived below for the case of symmetric systems will provide the locus of a curve in the p,ω plane which is sufficiently close to the actual escape region that it provides one good estimate for a bound on the location of part of the escape parameter zone. Another bounding curve for the escape zone is derived from considering a suitable subcritical bifurcation: around the region of interest it will turn out to be reasonably approximated by the bifurcation curves which arise in the linearized Mathieu equation version of Eq. (1.1) after a comparison with the usual vertical tangency condition discussed below. The escape zone ought to be bounded by these curves in the p,ω plane, as discussed in [2,3].

The harmonic balance method [9] is commonly used in most of the references cited above and is adopted here so that a solution of the form

$$\phi(t)=\phi_0+A\cos[\nu(\omega t+\beta)] \tag{2.1}$$

is assumed, where $\nu=\frac{1}{2}$ corresponds to the primary unstable zone around $\omega=2$ for the linearized Mathieu equation form of Eq. (1.1). For ease of notation, set

$$T=\tfrac{1}{2}(\omega t+\beta). \tag{2.2}$$

Inserting Eq. (2.1) into Eq. (1.1) and using the identities [[10], p. 361]

$$\cos(x\cos y)=J_0(x)+2\sum_{n=1}^{\infty}(-1)^n J_{2n}(x)\cos(2ny), \tag{2.3}$$

$$\sin(x\cos y)=2\sum_{n=1}^{\infty}(-1)^{n+1}J_{2n-1}(x)\cos[(2n-1)y], \tag{2.4}$$

where J_n denotes the Bessel function of the first kind of order n, gives

$$\begin{aligned}\tfrac{1}{4}\omega^2 A\cos T+\omega\xi A\sin T=&[1+p\cos(2T)\cos\beta+p\sin(2T)\sin\beta]\left[\sin\phi_0\left\{J_0(A)+2\sum_{n=1}^{\infty}(-1)^n J_{2n}(A)\cos(2nT)\right\}\right.\\&\left.+\cos\phi_0\left\{2\sum_{n=1}^{\infty}(-1)^{n+1}J_{2n-1}(A)\cos[(2n-1)T]\right\}\right]+a[1+p\cos(2T)\cos\beta+p\sin(2T)\sin\beta]\\&\times\left[\sin(2\phi_0)\left\{J_0(2A)+2\sum_{n=1}^{\infty}(-1)^n J_{2n}(2A)\cos(2nT)\right\}\right.\\&\left.+\cos(2\phi_0)\left\{2\sum_{n=1}^{\infty}(-1)^{n+1}J_{2n-1}(2A)\cos[(2n-1)T]\right\}\right].\end{aligned} \tag{2.5}$$

Following the procedure in [2], we collect together the terms involving $\cos T$, $\sin T$, and constants, and equate them to zero, ignoring the sinusoidal contributions from higher multiples of T. After some straightforward algebraic manipulations (involving trigonometric formulas for products of sines and cosines) this procedure leads to the following three equations:

$$\begin{aligned}&\tfrac{1}{4}A\omega^2-p\cos\beta\{\cos\phi_0[J_1(A)-J_3(A)]\\&\quad+a\cos(2\phi_0)[J_1(2A)-J_3(2A)]\}\\&\quad-2[\cos\phi_0 J_1(A)+a\cos(2\phi_0)J_1(2A)]=0,\end{aligned} \tag{2.6}$$

$$\begin{aligned}&\omega\xi A-p\sin\beta\{\cos\phi_0[J_1(A)+J_3(A)]\\&\quad+a\cos(2\phi_0)[J_1(2A)+J_3(2A)]\}=0,\end{aligned} \tag{2.7}$$

$$\begin{aligned}&\sin\phi_0\{J_0(A)-p\cos\beta J_2(A)\}\\&\quad+a\sin(2\phi_0)\{J_0(2A)-p\cos\beta J_2(2A)\}=0.\end{aligned} \tag{2.8}$$

These equations are analogous extensions to equations $(3a,b,c)$ in [2] and indeed collapse to these equations when a is set to zero.

Equation (2.8) can be split into the symmetric solution

$$\sin\phi_0=0, \tag{2.9}$$

and, assuming $\phi_0\approx 0$, an asymmetric solution

$$J_0(A)-p\cos\beta J_2(A)+2a\{J_0(2A)-p\cos\beta J_2(2A)\}=0. \tag{2.10}$$

For the symmetric solution $\phi_0=0$, Eqs. (2.6) and (2.7) can be suitably squared to eliminate the constant β, resulting in the relevant symmetric equation given by

$$\begin{aligned}&[\tfrac{1}{4}A\omega^2-2\{J_1(A)+aJ_1(2A)\}]^2+(\omega A\overline{\xi})^2\\&\quad-p^2[J_1(A)-J_3(A)+a\{J_1(2A)-J_3(2A)\}]^2=0,\end{aligned} \tag{2.11}$$

where

$$\overline{\xi}=\xi\frac{[J_1(A)-J_3(A)+a\{J_1(2A)-J_3(2A)\}]}{[J_1(A)+J_3(A)+a\{J_1(2A)+J_3(2A)\}]}. \tag{2.12}$$

For small $\beta\approx 0$ (corresponding to light damping) the asymmetric equation (2.10) reduces to

$$p=\frac{J_0(A)+2aJ_0(2A)}{J_2(A)+2aJ_2(2A)}. \tag{2.13}$$

The symmetry-breaking bifurcation in the ω, p plane can now be obtained by numerically solving the symmetric and asymmetric equations (2.11) and (2.13) simultaneously. We first substitute Eq. (2.13) for p in Eq. (2.11), choose fixed values of ξ and a, and set a starting value for ω in the vicinity of $\omega\approx 2$. Equation (2.11) is then solved numerically for A using a Newton-Raphson method initiated at $A=1$. The resulting value for A is then inserted into Eq. (2.13) to determine the corresponding value of p for the original starting value ω. This procedure is repeated through a range of values for ω and the resulting points (ω,p) provide the locus of the symmetry-breaking bifurcation curve in the ω, p plane for the chosen values of the constants ξ and a. For each a, if ξ is fixed, the curve forms one approximation for an expected lower bound to the escape region corresponding to the value of a. Examples of these curves are given in Fig. 1 (labeled on the right of the figure by S) for the case when $\xi=0.05$ and a

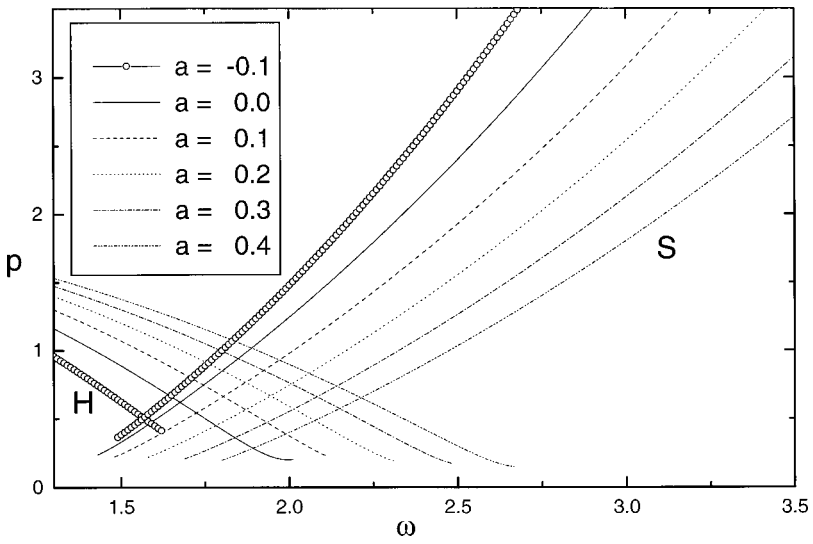

FIG. 1. The symmetry-breaking bifurcation curves S and the corresponding subcritical bifurcation curves H obtained by the harmonic balance method. The constant a takes the indicated values while ξ is set to 0.05 to allow a comparison with the results in Ref. [2] for the $a=0$ case. The escape region for each a is expected to be located above the relevant intersecting curves.

takes the indicated values; the $a=0$ case coincides with the symmetry-breaking curve depicted in [2].

The subcritical bifurcation is determined by the usual vertical tangency condition where $dA/d\omega=\infty$. If the left-hand side of Eq. (2.11) is defined to be the function f then $dA/d\omega=-f_\omega/f_A$ in terms of the partial derivatives of f. The standard series representations for Bessel functions [10] can be used to expand $f(A,\omega)$ around $A=0$. In this case, Eq. (2.11) can be expressed as

$$f(A,\omega)=A^2\{[\tfrac{1}{4}\omega^2-(1+2a)]^2+\omega^2\xi^2-\tfrac{1}{4}p^2(1+2a)^2\}+O(A^4)=0. \tag{2.14}$$

Hence, for small A,

$$\frac{dA}{d\omega}=-\frac{f_\omega}{f_A}=\frac{-\tfrac{1}{2}A\omega[\tfrac{1}{4}\omega^2-(1+2a)+2\xi^2]}{[\tfrac{1}{4}\omega^2-(1+2a)]^2+\omega^2\xi^2-\tfrac{1}{4}p^2(1+2a)^2}+O(A^3). \tag{2.15}$$

Hence $dA/d\omega=\infty$ whenever

$$[\tfrac{1}{4}\omega^2-(1+2a)]^2+\omega^2\xi^2-\tfrac{1}{4}p^2(1+2a)^2=0. \tag{2.16}$$

This equation is expected to provide a reasonable approximation to another lower bound for the escape region; it can also be obtained by considering the linearized version of Eq. (1.1) in the form of the Mathieu equation (see for example [[11], p. 260] when ω and the other constants are appropriately redefined). Examples of these curves appear in Fig. 1 (labeled to the left of the figure by H) for $\xi=0.05$ and the indicated values of a. For each given value of a the corresponding H and S curves combined as in Fig. 1 form good approximate lower bounds for the anticipated escape region in the ω, p plane: this is certainly the case for $a=0$ as discussed by Clifford and Bishop [2].

III. APPLICATION

An application of the results derived above may be made for Eq. (2.10) in the paper by Stewart, Carlsson, and Leslie [12],

$$B_3\phi_{zz}-2\lambda_5\phi_t-\epsilon_0\epsilon_a E_0^2(\sin\alpha\cos\theta+\cos\alpha\sin\theta\cos\phi)\cos\alpha\sin\theta\sin\phi=0. \tag{3.1}$$

This, and similar equations with sine terms, may be found throughout the smectic-C liquid-crystal literature (see Cladis and van Saarloos [13], Schiller, Pelzl, and Demus [14], the work contained in Maclennan, Clark, and Handschy [15] and the references in [1]). Smectic liquid crystals are layered anisotropic fluids, the physics of which can be found in great detail in the book by de Gennes and Prost [16]. The average molecular alignment in a liquid crystal is described by the unit vector **n**, commonly called the director. Here $\phi=\phi(z,t)$ is the orientation angle of the usual c director which, by the physics of smectic C [16], allows a complete description of the director **n** within any smectic-C liquid-crystal sample. The quantity $B_3>0$ is an elastic constant and $\lambda_5>0$ is a smectic viscosity coefficient. The electric field $\mathbf{E}=E_0(\cos\alpha,0,\sin\alpha)$ makes a constant angle α relative to the equidistant planes of the smectic layers aligned parallel with the xy plane. The fixed smectic tilt angle θ is the angle the director **n** makes relative to the layer normal (0, 0, 1). The magnitude of the electric field is E_0, ϵ_0 is the (positive) permittivity of free space and ϵ_a is the dielectric anisotropy of the liquid crystal, which may be positive or negative. Equation (3.1) has been derived in [12] from the nonlinear continuum theory for smectic-C liquid crystals developed by Leslie, Stewart, and Nakagawa [17].

For $\epsilon_a>0$ and E_0 set to a constant value there is a well-known traveling wave solution to Eq. (3.1), namely [1,12–15],

$$\phi(z,t)=2\arctan[\exp(b\tau)], \tag{3.2}$$

where

$$b=E_0(\epsilon_0\epsilon_a)^{1/2}B_3^{-1/2}\cos\alpha\sin\theta, \tag{3.3}$$

$$\tau = z - ct - z_0, \tag{3.4}$$

$$c = \tfrac{1}{2} E_0 (B_3 \epsilon_0 \epsilon_a)^{1/2} \lambda_5^{-1} \sin\alpha \cos\theta, \tag{3.5}$$

with z_0 being an arbitrary constant. The solution $\phi(z,t)$ travels from π to 0 as t increases. This form of solution occurs frequently and has been exploited and developed on various occasions in the context of smectic liquid crystals [18,19].

To investigate the behavior when $E_0 = E_0(t)$ we suppose that for some positive constant E_0

$$E_0(t) = E_0[1 + \tfrac{1}{2}\epsilon\cos(\omega t)] \quad 0 < \epsilon \ll 1. \tag{3.6}$$

This models a perturbation to the constant electric field case via a static field which is augmented by a small amplitude oscillating field; ω is the frequency of the superimposed field and ϵ is a small parameter. Given the form of Eq. (3.6) it is observed that [12]

$$\epsilon\cos(\omega t) \approx \epsilon\cos\left(\frac{\omega}{c}\tau\right), \tag{3.7}$$

whenever

$$|z - z_0|\frac{\omega}{c} < \epsilon, \tag{3.8}$$

that is, whenever the solution is investigated sufficiently near any initially chosen arbitrary point z_0. For a given range of values for ω it can always be ensured that the inequality in Eq. (3.8) holds: we are principally interested in the large τ behavior. Consequently, we may consider

$$E_0^2(t) \approx E_0^2\left[1 + \epsilon\cos\left(\frac{\omega}{c}\tau\right)\right]. \tag{3.9}$$

Motivated by the traveling wave solution (3.2) to Eq. (3.1) and the general form of the equation discussed in Sec. II, we suppose that for electric fields satisfying the approximations in Eq. (3.9) we can choose to examine solutions of the type

$$\phi = \hat{\phi}(d\tau) + \pi, \tag{3.10}$$

$$d = b\sqrt{\tan\alpha\cot\theta}, \tag{3.11}$$

where b and τ are defined as above in Eqs. (3.3) and (3.4). Substituting equations (3.9) and (3.10) into Eq. (3.1) gives

$$\hat{\phi}_{\tau\tau} + 2\xi\hat{\phi}_\tau + [1 + \epsilon\cos(\bar{\omega}\tau)][\sin\hat{\phi} + a\sin(2\hat{\phi})] = 0, \tag{3.12}$$

where, for notational convenience,

$$\xi = \tfrac{1}{2}\sqrt{\tan\alpha\cot\theta}, \tag{3.13}$$

$$\bar{\omega} = \frac{\omega}{c}, \tag{3.14}$$

$$a = -\tfrac{1}{2}\cot\alpha\tan\theta = -\tfrac{1}{8}\xi^{-2}. \tag{3.15}$$

The variable $\bar{\omega}$ involves many of the problem-dependent constant parameters via c defined in Eq. (3.5), including the magnitude of the static electric field contribution. For a given physical situation, α and θ are chosen known fixed parameters while the electric field can be varied. This means that varying the frequency and magnitude of the electric field contributions can be accommodated by only needing to consider the effect of varying $\bar{\omega}$ and ϵ. Equation (3.12) is of the same form as Eq. (1.1) with ϵ (the magnitude of the oscillating field contribution) playing the rôle of p.

For $\epsilon_a < 0$ it can be supposed again that a solution similar to Eq. (3.10) may be appropriate when $\epsilon \neq 0$, given the results above for $\epsilon_a > 0$. We suppose in this case that

$$\phi = \hat{\phi}(d\tau), \tag{3.16}$$

with d again given by Eq. (3.11), except that in this case we replace ϵ_a in Eqs. (3.3) and (3.5) by $-\epsilon_a > 0$. Setting Eq. (3.16) into Eq. (1.1) gives Eq. (3.12) as before with ξ and $\bar{\omega}$ as defined in Eqs. (3.13) and (3.14) but with a replaced by

$$a = \tfrac{1}{2}\cot\alpha\tan\theta = \tfrac{1}{8}\xi^{-2}. \tag{3.17}$$

From the preceding paragraphs we are now in a position to employ Eq. (3.12) and the results of Sec. II for $a < 0$ and $a > 0$ corresponding to the cases $\epsilon_a > 0$ and $\epsilon_a < 0$, respectively. In both cases, a and ξ are related to each other by Eqs. (3.17) and (3.15). For illustrative examples we consider graphs in the $\bar{\omega}, \epsilon$ plane when a is set to some particular negative or positive values. The method used to obtain Fig. 1 can be repeated to obtain Fig. 2 below for Eq. (3.12), the main difference being the dependence of ξ upon a. The plots in Fig. 2 have been calculated for the bifurcation curves in the $\bar{\omega}, \epsilon$ plane for the values $a = -0.1$, 0.3, 0.5, and 0.7, in order that the values for ξ remain relatively small: the approximate corresponding ξ values are 1.118, 0.645, 0.5, and 0.425, respectively. Numerical evidence tends to suggest that the curves remain similar in form to those in Fig. 1 provided $|a|, |\xi| \lesssim 0.75$. As in Fig. 1, the symmetry-breaking bifurcation curves are labeled S and the subcritical bifurcation curves are labeled H. For $a = -0.1$ it is seen from the figure that the upper of the two corresponding curves is the subcritical bifurcation curve, extended further to the right of $\bar{\omega} = 2$ than in Fig. 1; this curve lies above the symmetry-breaking bifurcation curve which, unlike Fig. 1, does not intersect the subcritical bifurcation curve for $1 \leqslant \omega \leqslant 3.5$. There is a similar scenario for the $a = 0.3$ case in Fig. 2. This is due to ξ being much larger than the value considered for Fig. 1. However, for $a = 0.5$ and 0.7, ξ becomes smaller and the symmetry-breaking and subcritical bifurcation curves intersect as shown in Fig. 2 in a similar way to those displayed in Fig. 1. It is anticipated that any escape region will be located above these curves in the $\bar{\omega}, \epsilon$ plane.

From Fig. 2 it can be seen that escape behavior ought not to be expected for $0 \leqslant \epsilon \lesssim 1$ for the given ranges of a. Nevertheless, this does not preclude the existence of transient chaos. This is certainly the case for some nonlinear oscillator equations where, for example, a Melnikov-type analysis can reveal a further boundary, the Melnikov curve, in the $\bar{\omega}, \epsilon$ plane which lies below the symmetry-breaking and subcritical bifurcation curves; transient chaos may occur for parameters in the region above the Melnikov curve. Some examples of this behavior can be found in the review paper by Szemplinska-Stupnicka [20]. Melnikov boundaries were de-

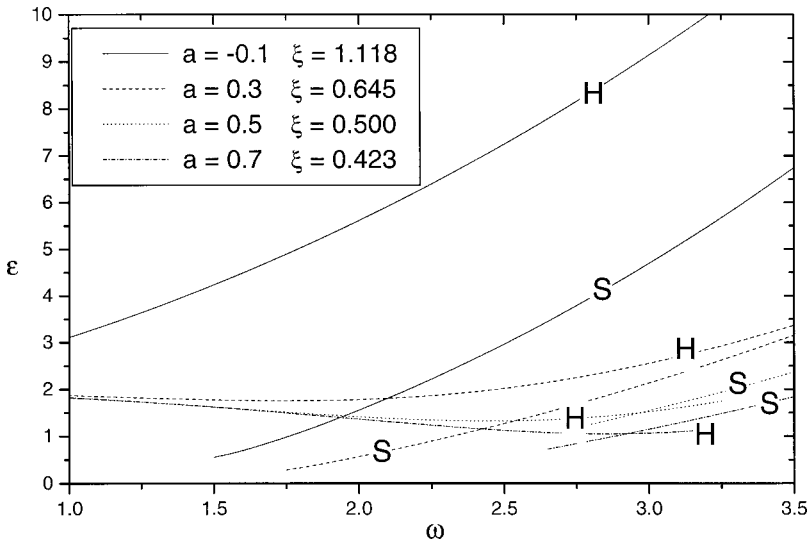

FIG. 2. The symmetry-breaking bifurcation curves *S* and the corresponding subcritical bifurcation curves *H*, obtained by the harmonic balance method for Eq. (3.12). The parameters a and ξ are linked according to Eq. (3.15) when $a<0$ and to Eq. (3.17) when $a>0$. As in Fig. 1, the escape region is always expected to be located above the relevant curves.

termined by Stewart *et al.* [12] for a slightly different form of perturbation to Eq. (3.1) and its known traveling-wave solution (3.2). As a result of the differences between these perturbations, a direct comparison of the results in [12] with those presented here is not feasible, although both sets of results qualitatively agree that complex nonlinear behavior is to be anticipated as ϵ increases, that is, as the magnitude of the oscillating electric field contribution increases. This is similar to the situation for various types of nonlinear oscillators subjected to a driving periodic force such as $F\cos(\omega t)$: complex behavior patterns can emerge as F increases leading to chaos and/or escape regions in the ω, F plane (see, for example, Fig. 10 in [20]). The choice of perturbation introduced here has the advantage over that in [12] of having fewer assumptions imposed upon the proposed solution. The techniques used in this present paper are therefore more general in relation to Eq. (3.1) despite the rather basic approximations in Eqs. (3.6)–(3.9) used for the special perturbation to the known traveling-wave solution described here and it is hoped that this simple example will encourage more extensive numerical analysis of Eq. (1.1) than is currently available in the literature.

IV. CONCLUSIONS

The theory and results expounded by Clifford and Bishop [2] for the case of equation (1.1) with $\xi>0$ fixed and $a=0$ have been extended in Sec. II to incorporate an additional sinusoidal term when $a\neq 0$. A general method has been introduced to produce symmetry-breaking and subcritical bifurcation curves in the ω,ϵ plane around the primary unstable zone near $\omega\approx 2$. Examples for various values of a are displayed in Fig. 1 for $\xi=0.05$. These intersecting curves, for each a, represent lower bounds on the location of any anticipated escape parameter region in the ω,ϵ plane. The special case of $a=0$ coincides with the results in [2].

The motivation for investigating equation (1.1) when $a\neq 0$ arises from a well-known dynamic equation from the smectic liquid-crystal literature, namely, Eq. (3.1). This equation has a double sine-Gordon-type nonlinearity entering through two sinusoidal terms. In Sec. III a special perturbation to this equation involving an oscillating electric field term led, by means of some basic approximations and assumptions introduced in Eqs. (3.6)–(3.9), to Eq. (3.12) which then allowed a direct application of the theory derived in Sec. II. The resulting bifurcation curves are plotted in Fig. 2. For this particular application ξ and a are related to each other via Eqs. (3.15) and (3.17), depending upon the sign of the constant dielectric anisotropy ϵ_a of the liquid-crystal material (which could be either positive or negative [16]). The results clearly have an impact upon the interpretation of the orientation of the *c* director (and hence the average molecular alignment denoted by the usual director **n**) in smectic liquid crystals via the phase angle ϕ, especially when the possibility of large-time chaotic behavior may be present for parameters lying within the escape zones. These results for liquid crystals bear some resemblance to those for nonlinear oscillators with a periodic driving force [20], as mentioned briefly in Sec. III. Further, the application of the results presented here in Sec. III agrees qualitatively with those presented elsewhere [12] for Eq. (3.1) when E_0 is given by Eq. (3.6) in that as the amplitude of the oscillatory field contribution increases, there is an increased opportunity for complex nonlinear behavior.

The preliminary results presented here will hopefully stimulate interest in carrying out more detailed numerical work in an attempt to more accurately locate the escape regions for Eq. (1.1). The boundary curves presented here will guide numerical experiments by giving appropriate areas in the frequency and amplitude parameter space for investigations to begin.

[1] I. W. Stewart, IMA J. Appl. Math. **61**, 47 (1998).
[2] M. J. Clifford and S. R. Bishop, J. Sound Vib. **172**, 572 (1994).
[3] D. Capecchi and S. R. Bishop, Dyn. Stability Systems **9**, 123 (1994).
[4] M. J. Clifford and S. R. Bishop, Phys. Lett. A **184**, 57 (1993).

[5] S. R. Bishop and M. J. Clifford, Eur. J. Mech. A/Solids **13**, 581 (1994).
[6] S. R. Bishop and M. J. Clifford, Chaos, Solitons Fractals **7**, 1537 (1996).
[7] S. R. Bishop and M. J. Clifford, J. Sound Vib. **189**, 142 (1996).
[8] M. J. Clifford (private communication).
[9] A. H. Nayfeh and D. T. Mook, *Non-Linear Oscillations* (Wiley, New York, 1979).
[10] *Handbook of Mathematical Functions*, edited by M. Abramowitz and I. A. Stegun (Dover, New York, 1970).
[11] D. W. Jordan and P. Smith, *Nonlinear Ordinary Differential Equations*, 2nd ed. (Clarendon, Oxford, 1987).
[12] I. W. Stewart, T. Carlsson, and F. M. Leslie, Phys. Rev. E **49**, 2130 (1994).
[13] P. E. Cladis and W. van Saarloos, in *Solitons in Liquid Crystals*, edited by L. Lam and J. Prost (Springer-Verlag, New York, 1992), pp. 110–150.
[14] P. Schiller, G. Pelzl, and D. Demus, Liq. Cryst. **2**, 21 (1987).
[15] J. E. Maclennan, N. A. Clark, and M. A. Handschy, in *Solitons in Liquid Crystals*, edited by L. Lam and J. Prost (Springer-Verlag, New York, 1992), pp. 151–190.
[16] P. G. de Gennes and J. Prost, *The Physics of Liquid Crystals* (Clarendon, Oxford, 1993).
[17] F. M. Leslie, I. W. Stewart, and M. Nakagawa, Mol. Cryst. Liq. Cryst. **198**, 443 (1991).
[18] W. van Saarloos, M. van Hecke, and R. Holyst, Phys. Rev. E **52**, 1773 (1995).
[19] I. W. Stewart, Phys. Rev. E **57**, 5626 (1998).
[20] W. Szemplinska-Stupnicka, Nonlinear Dyn. **7**, 129 (1995).